Biointerface Research in Applied Chemistry
Platinum Open Access Journal (ISSN: 2069-5837)

*Article*
**Volume 12, Issue 5, 2022, 6100 - 6113**
https://doi.org/10.33263/BRIAC125.61006113

# Effect of New Thalidomide Analogs in Acute Kidney Injury on Rats

**Ahmed Fadda [1,*], Mohamed Youssif [2], Safaa Derbala [3], Yasmin Tag [4], Hala Refaat [5]**

1 Department of Chemistry, Faculty of Science, Mansoura University, ET-35516 Mansoura, Egypt; afadda50@yahoo.com (A.F.);
2 Medical Experimental Research Centre, Faculty of Medicine, Mansoura University, ET-35516 Mansoura, Egypt; m.13579youssef@gmail.com (M.Y.);
3 Uorology and Nephrology Centre, Mansoura University, ET-35516 Mansoura, Egypt; safaaderbala@yahoo.com (S.D.);
4 Oral Biology Department, Faculty of Oral and Dental medicine, Delta University for Science and Technology, Mansoura, Egypt; yasmintag21@yahoo.com (Y.T.);
5 Department of Chemistry, Faculty of Science, Arish University, 45511 Al-Arish, Egypt; hala7223530@hotmail.com (H.R.);
* Correspondence: afadda50@yahoo.com (A.F.);

Scopus Author ID 7005134210
**Received: 14.07.2021; Revised: 22.09.2021; Accepted: 26.09.2021; Published: 4.11.2021**

**Abstract:** Renal ischemia/reperfusion (I/R) injury contains multiple mechanisms involving an excessive amount of ROS that causes oxidative stress, inflammation, and rapid kidney dysfunction. This work aimed to study the ability of thalixisostere **3f** on angiogenesis and antioxidant effect in I/R. There was a significant decrease in VEGF from thalix and modified thalixisostere **3f** groups as compared with that of a negative control group ($P < 0.001$). There was a significant decrease in the mean concentration of MDA in kidney tissue obtained from thalix and thalixisostere **3f** groups as compared with that of a positive control group ($P < 0.001$). There was a significant increase in the mean concentrations of SOD and GSH in kidney tissue of group's thalix and thalixisostere **3f** groups as compared with that of a positive control group. We found that thalixisostere **3f** is more effective than thalix in inhibiting the expression VEGF as pro-angiogenic factors. Molecular docking study indicated that the proper recognition of the inhibitor thalix-isostere with the conserved amino acid residues at the binding active site of VEGFR2 as one of the important enzymes to be targeted as part of antiangiogenic anticancer.

**Keywords:** cyclic imides; ischemic kidney; thalidomide; thalixisostere.



## 1. Introduction

Ischemia and/or reperfusion (I/R) is one of the main factors participating in acute kidney injury [1]. It can happen as a result of systemic hypoperfusion (e.g., shock) with following circulatory resuscitations and tentative stopping of renal blood supply, e.g., in renal transplantation, partial kidney resection, and aortic cross-clamping [2]. The renal I/R injury is followed by complex mechanisms, including reactive oxygen species (ROS), ATP depletion, accumulation of intracellular $Ca^{2+}$, mitochondrial dysfunction, multiple enzyme method effects, and proinflammatory cytokine production [3]. Multiple series of cellular reactions that finally produce renal cell death result from the harmful effect of I/R. However, experimental results recommend that apoptosis, hypoxia, oxidative stress, endothelial dysfunction, and inflammatory response are essential in renal dysfunction through ischemic reperfusion (IR)

conditions [4]. Oxidative stress and inflammation are found to be interconnected and thus prove to be the main providers of RIRI [5]. Recovery of kidney function after I/R injury based on injured cell replacement or renewal and protection from programmed cell death (apoptosis) [6]. In order to prevent irreversible tissue injury, blood flow restoration to ischaemic organs is essential. Although tissue injury may be induced by ischemia, reperfusion persist may also induce tissue injury [3, 7].

Vascular endothelial growth factor (VEGF) is thought to be one of the essential angiogenic factors, which can enhance the production of new blood vessels and lymphatic vessels [8]. VEGF has a number of different physiological organisms. For example, VEGF has a selective effect of increased endothelial cell mitosis and enhancing angiogenesis and endothelial cell reproduction. Also, VEGF can strengthen blood vessels by growing capillary permeability and thus enhancing plasma proteins' extravasations and other macromolecules. On the other hand, it raises the deposition to the extravascular matrix and provides nutrition to create novel capillary networks. So, VEGF is one of the essential growth factors for angiogenesis, which has a significant role in blood vessels production [9]. Thalidomide (thalix), was utilized as a sedative and anti-nausea drug in the 1950s but was prevented due to teratogenicity [10]. Thalidomide is anti-inflammatory and antiangiogenic. It has been shown to generate reactive oxygen species (ROS) [11]. In 1994, thalidomide became the focus of intense oncological research after its antiangiogenic properties. Its antiangiogenic effects have led to its assumption as an anticancer agent [12]. The above-mentioned biological interest data prompted us to find a new class of heterocyclic imide, structural analogs of the systemic thalidomide, and matching the effects of it on the renal dysfunction and injury affected by I/R of the kidney of the mouse in vivo when given as treatment (thalidomide and thalixisostere) for 3 days or when given for 7 days and for 14 days to reperfusion of the ischemic kidney.

## 2. Materials and Methods

All spectroscopic data were recorded according to the methods previously reported [13].

### *2.1. Synthesis of cyclic imide derivatives (3a-f).*

***General procedure***

Equimolar amounts of 6-aminouracil (1.27 g, 10 mmol) and phthalic anhydride (2.57 g, 10 mmol) and/or 3-nitrophthalic anhydride (3.02 g, 10 mmol) and/or 4-nitrophthalic anhydride (3.02 g, 10 mmol) and/or 1,2,4-benzenetricarboxlic anhydride (3.01 g, 10 mmol) and/or tetrabromophthalic anhydride (5.68 g, 10 mmol) and/or quinolinic anhydride (1.49 g, 10 mmol) in the presence of freshly fused sodium acetate (1.64 g, 20 mmol) were fused at 150 $^{o}$C in a silicon oil bath. The reaction mixture was then left to cool at room temperature; ethanol was added to the mixture. The formed solids were collected by filtration, washed with water, dried, and crystallized from EtOH to give compounds **3a-f**.

2.1.1. 2-(2,6-Dioxo-1,2,3,6-tetrahydropyrimidin-4-yl)isoindoline-1,3-dione 3a.

White powder; yield (86%); mp> 300$^{o}$C; IR (KBr): v/cm$^{-1}$= 3215 (2NH), 1724, 1690 (4C=O); $^{1}$H NMR (DMSO-$d_6$) δ (ppm): 4.86 (s, 1H, C5-pyrimidine ring), 7.68 (s, 4H, Ar-H), 10.45, 10.87 (s, 2H, 2NH, $D_2O$ exchangeable);$^{13}$C NMR (125 MHz, DMSO-$d_6$) δ (ppm): 76.7, 124.7 (2C), 130.3 (2C), 132.6 (2C), 151.8, 163.2, 164.5 (2C), 166.9; MS (EI, 70 eV): *m/z* (%)

257 ($M^+$, 34.16), 215 (21.01), 207 (100.00), 157 (36.38), 125 (27.70), 100 (44.05); Anal. Calcd. For $C_{12}H_7N_3O_4$ (257.21): C, 56.04; H, 2.74; N, 16.34; Found: C, 56.11; H, 2.83; N, 16.40%.

2.1.2. 2-(2,6-Dioxo-1,2,3,6-tetrahydropyrimidin-4-yl)-4-nitroisoindoline-1,3-dione 3b.

Pale yellow powder; yield (84%); mp> 300ºC; IR (KBr): v/$cm^{-1}$= 3214 (2NH), 1725, 1694 (4C=O); $^1$H NMR (DMSO-$d_6$) δ (ppm): 3.87 (s, 1H, C5-pyrimidine ring), 8.16 (m, 1H, Ar-H), 8.45 (d, 1H, *J* = 8.0 Hz, Ar-H), 8.63 (d, 1H, *J* = 8.0 Hz, Ar-H), 10.41, 10.64 (s, 2H, 2NH, $D_2O$ exchangeable); $^{13}$C NMR (125 MHz, DMSO-$d_6$) δ (ppm): 76.8, 127.1, 128.4, 130.5, 133.6, 134.3, 146.8, 151.2, 163.3, 164.1, 165.6, 166.7; MS (EI, 70 eV): *m/z* (%) 301 ($M^+$-1, 30.31), 279 (100.00), 275 (24.11), 215 (25.26), 155 (49.52), 139 (58.19); Anal. Calcd. For $C_{12}H_6N_4O_6$ (302.20): C, 47.69; H, 2.00; N, 18.54; Found: C, 47.72; H, 2.06; N, 18.61%.

2.1.3. 2-(2,6-Dioxo-1,2,3,6-tetrahydropyrimidin-4-yl)-5-nitroisoindoline-1,3-dione 3c.

Yellow powder; yield (81%); mp> 300ºC; IR (KBr): v/$cm^{-1}$= 3222 (2NH), 1731, 1689 (4C=O); $^1$H NMR (DMSO-$d_6$) δ (ppm): 4.88 (s, 1H, C5-pyrimidine ring), 8.24 (d, 1H, *J* = 8.0 Hz, Ar-H), 8.43 (s, 1H, Ar-H), 8.65 (d, 1H, *J* = 8.0 Hz, Ar-H), 10.45, 10.68 (s, 2H, 2NH, $D_2O$ exchangeable); $^{13}$C NMR (125 MHz, DMSO-$d_6$) δ (ppm): 76.3, 122.4, 127.4, 130.1, 131.7, 136.2, 148.6, 151.4, 163.2, 164.5, 165.8, 166.7; MS (EI, 70 eV): *m/z* (%) 302 ($M^+$, 5.91), 284 (100.00), 257 (50.84), 231 (10.47), 181 (9.04), 115 (60.22); Anal. Calcd. For $C_{12}H_6N_4O_6$ (302.20): C, 47.69; H, 2.00; N, 18.54; Found: C, 47.74; H, 2.04; N, 18.62%.

2.1.4. 2-(2,6-Dioxo-1,2,3,6-tetrahydropyrimidin-4-yl)-1,3-dioxoisoindoline-5-carboxylic acid 3d.

Pale yellow powder; yield (80%); mp> 300ºC; IR (KBr): v/$cm^{-1}$= 3242 (2NH), 1725, 1697 (4C=O); $^1$H NMR (DMSO-$d_6$) δ (ppm): 4.85 (s, 1H, C5-pyrimidine ring), 8.12 (d, 1H, *J* = 8.0 Hz, Ar-H), 8.46 (s, 1H, Ar-H), 8.63 (d, 1H, *J* = 8.0 Hz, Ar-H), 10.42, 10.67 (s, 2H, 2NH, $D_2O$ exchangeable), 12.63 (s, 1H, OH, $D_2O$ exchangeable); $^{13}$C NMR (125 MHz, DMSO-$d_6$) δ (ppm): 76.2, 124.3, 130.4, 131.0, 133.2, 134.8, 136.4, 151.2, 163.4, 164.6, 165.8, 166.4, 170.1; MS (EI, 70 eV): *m/z* (%) 301 ($M^+$, 7.10), 270 (32.83), 231 (41.81), 192 (39.91), 183 (35.70), 155 (43.05), 135 (58.68); Anal. Calcd. For $C_{13}H_7N_3O_6$ (301.21): C, 51.84; H, 2.34; N, 13.95; Found: C, 51.90; H, 2.41; N, 13.98%.

2.1.5. 4,5,6,7-Tetrabromo-2-(2,6-dioxo-1,2,3,6-tetrahydropyrimidin-4-yl)isoindoline-1,3-dione 3e.

Yellow powder; yield (88%); mp> 300ºC; IR (KBr): v/$cm^{-1}$= 3214 (2NH), 1726, 1690 (4C=O); $^1$H NMR (DMSO-$d_6$) δ (ppm): 4.84 (s, 1H, C5-pyrimidine ring), 10.42, 10.76 (s, 2H, 2NH, $D_2O$ exchangeable); $^{13}$C NMR (125 MHz, DMSO-$d_6$) δ (ppm): 76.7, 124.2 (2C), 129.5 (2C), 138.8 (2C), 151.2, 163.1, 165.6 (2C), 166.4; MS (EI, 70 eV): *m/z* (%) 573 ($M^+$+1, 28.88), 572 ($M^+$, 36.52), 512 (63.52), 461 (34.96), 338 (28.65), 299 (100.00), 199 (49.71); Anal. Calcd. For $C_{12}H_3Br_4N_3O_4$ (572.79): C, 25.16; H, 0.53; N, 7.34; Found: C, 25.22; H, 0.55; N, 7.42%.

2.1.6. 6-(2,6-Dioxo-1,2,3,6-tetrahydropyrimidin-4-yl)-5H-pyrrolo[3,4-b]pyridine-5,7(6H)-dione 3f.

Buff powder; yield (86%); mp 238-240ºC; IR (KBr): v/cm$^{-1}$= 3268 (2NH), 1725, 1642 (4C=O); $^{1}$H NMR (DMSO-$d_6$) δ (ppm): 5.76 (s, 1H, C5-pyrimidine ring), 7.38-9.12 (m, 3H, Ar-H), 10.21, 10.68 (s, 2H, 2NH, $D_2O$ exchangeable); $^{13}$C NMR (125 MHz, DMSO-$d_6$) δ (ppm): 76.5, 124.6, 128.5, 131.4, 148.8, 150.6, 152.4, 160.3, 163.2, 167.4, 168.7; MS (EI, 70 eV): *m/z* (%) 259 ($M^+$+1, 54.50), 193 (100.00), 168 (36.40), 150 (90.90), 128 (63.60), 112 (100.00); Anal. Calcd. For $C_{11}H_6N_4O_4$ (258.19): C, 51.17; H, 2.34; N, 21.70; Found: C, 51.26; H, 2.39; N, 21.77%.

*2.2. Animals.*

Fifty-four male Sprague-Dawley rats weighing (201.0± 10.5) g 3-4 Months old were purchased from the Medical Experimental Research Center (MERC) animal labs. Rats were allowed access to food and water at the Medical Experimental Research Center (MERC) animal labs. It was assumed that all laboratory animals had the standard diet and clean water freely during the experiment. Ventilation was suitable in the feeding room, with the natural lighting day and night. The culture temperature was preserved at 18–25 °C. In the present study, there were ten mice groups.

2.2.1. Animal model.

After one week of adaptive feeding, 3-4 month male Sprague-Dawley rats were randomly divided into 9 groups, (1) Negative control group, (2) Positive ischemic/reperfusion control group mice suffered 45 min left renal ischemia tracked by clamp relief (3) thalix treated ischemic/ reperfusion group, rats obtained thalidomide (thalix) (1000 IU/kg, SC) 24 h before the operative method and continued daily till the day of sacrifice; and from (4) to (9) thalixisostere from **3a to 3f** treated ischemic/ reperfusion group rats received thalixisostere from **3a to 3f** (1000 IU/kg, SC) 24 h before the operative method and continued every day till the day of sacrifice. All rats with renal ischemic/reperfusion were subjected to serum analysis before surgery and 3days after renal ischemia/Reperfusion induction (n=6) for each group.

2.2.2. Biochemical parameters.

Blood samples were taken before surgery at the end of the reperfusion period and 3days after renal ischemia for biochemical tests: Blood samples for creatinine and urea were measured using a colorimetric assay.

2.2.3. Estimation of lipid peroxidation, antioxidant enzymes, and non-enzymatic antioxidant in kidney tissues.

Kidney tissues, harvested at 3days after ischemia, were kept in cold conditions. It was cut using a surgical scalpel to fine slices in the chilled 0.25 M sucrose and quickly flushed onto the filter paper. The tissue was chopped and homogenized in 10 mm Tris-HCl buffer, pH 7.4 (10 % w/v), with 25 strokes of Teflon pestle from the glass mixer at 2500 rpm. The clear supernatant was used for lipid peroxidation (MDA), antioxidant enzyme Superoxide dismutase (SOD), and low-glutathione (GSH) using a colorimetric group (Bio- Diagnostics, Dokki, Giza, Egypt) according to the manufacturer's instructions for commercially available kits.

2.2.4. Estimation of vascular endothelial growth factor.

Bio-Plex Pro human angiogenesis array for VEGF was run according to the manufacturer's instructions (Cat # M50007W214 Bio-Rad Laboratories, USA), which quantifies multiple protein bio-factors.

2.2.5. Methodology of molecular docking.

In the present work, the 3D structure of the VEGFR-2 enzyme was taken from a Protein Data Bank entry (PDB entry: 4ASD) co-crystalized with sorafenib as a ligand. The novel derivatives were built and optimized at the ChemDraw professional 2016. The optimized structures were then docked and analyzed using MOE software to determine specific interactions between ligands and essential amino acids within the active site of the VEGFR-2 enzyme.

*2.3. Principle.*

Antiangiogenesis activities studies used the 3-D crystallographic VEGFR2 (4ASD) to explore the thalidomide and its structural relevant analog recognition in the active site as a potential antioxidant.

*2.4. Statistical analysis.*

All values described in the text and figures are expressed as mean ± standard deviation (SD) for *N* observations. One-way analysis of variance (ANOVA) with the Bonferroni post hoc test was performed using SPSS version 19 for Windows. *P* values of less than 0.05were considered to be significant.

## 3. Results and Discussion

*3.1. Results.*

3.1.1. Chemistry.

The newly synthesized cyclic imide derivatives 3a-f based on the fusion of anhydride derivatives 1a-f with 6-aminopyrimidine-2,4(1H,3H)-dione (2) in the presence of freshly fused sodium acetate (Scheme 1).

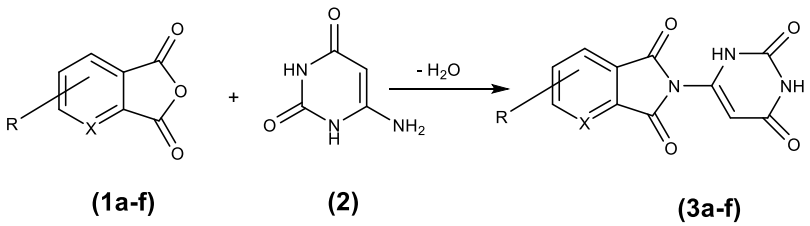


**(1a-f)** **(2)** **(3a-f)**

**1 and 3,a,** X= C, R= H, **1 and 3,b,** X= C, R= 3-$NO_2$, **1 and 3,c,** X= C, R= 4-$NO_2$,
**1 and 3,d,** X= C, R= 4-COOH, **1 and 3,e,** X= C, R= 3,4,5,6-Br, **1 and 3,f,** X= N, R= H

**Scheme 1.** Synthesis of cyclic imide derivatives.

Structures of the products **3a-f** were confirmed by both elemental and spectral data. The IR spectra of compounds **3a-f** showed the characteristic absorption bands in the region 3214-

3381 $cm^{-1}$ corresponding to the stretching vibration of the two NH groups. Also, the strong frequency region of the spectra showed the absorption bands at 1690-1679 $cm^{-1}$ due to the stretching vibrations of the four CO groups. Also, the mass spectroscopic measurements of compounds **3a-f** showed the molecular ion peaks at *m/z* = 257 ($M^+$), 301 ($M^+$-1), 302 ($M^+$), 301($M^+$), 573 ($M^+$+1) and 259 ($M^+$+1), respectively, which are in agreement with their suggested structures. $^1$H NMR spectrum of structure **3f** as an example revealed singlet signals at δ 4.85, 10.51, and 10.89 ppm assignable to C-$H_5$ of the pyrimidine ring and two NH protons.

The formation of cyclic imides **3a-f** can be postulated according to the following mechanism (Scheme 2):

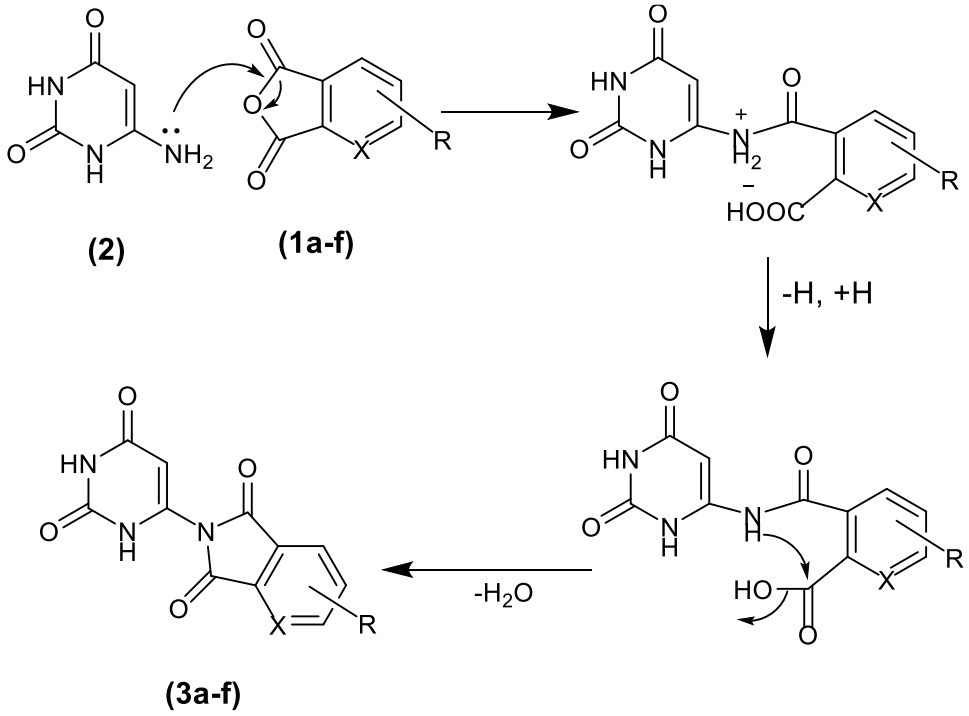


**Scheme 2.** The mechanism of the formation of cyclic imide derivatives.

3.1.2. Pharmacological.

Kidney renal I/R injury is a difficult inflammatory method in which it is functional and morphologically destroyed through the ischaemic stage and undergoes additional injury through reperfusion.

In the current study, the effect of pretreatment with thalix and thalixisosteres **3a-f** on renal function, angiogenesis VEGF, MDA (Malondialdehyde) (a marker of lipid peroxidation), SOD (Superoxide dismutase) (a marker of antioxidant enzyme), and GSH (Glutathione) (a marker of non-enzymatic antioxidant) were investigated.

3.1.2.1. The effect of thalixisosteres3a--3f on body weight:

As in Figure 1, there was an insignificant change in the body weight in all groups before (P = 0.427). There was a significant decrease in all I/R groups' final body weight compared to a negative control group (P=0.01).

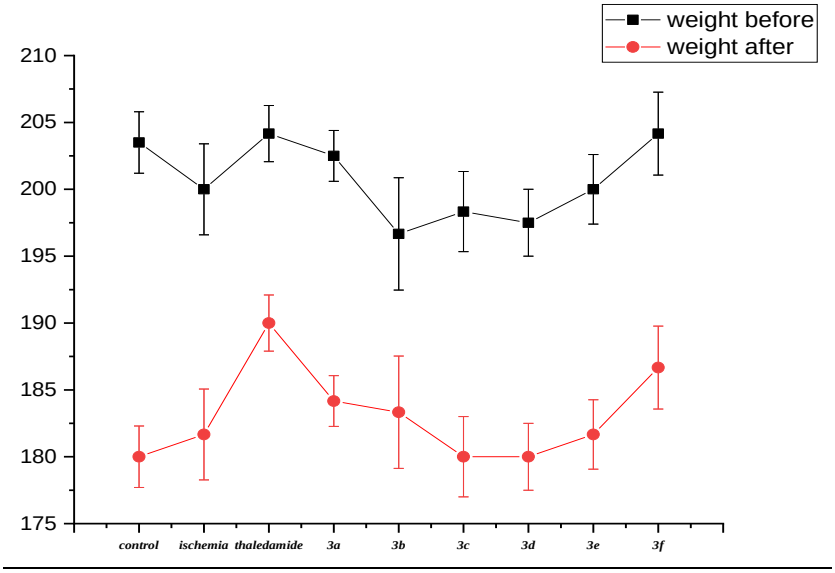


**Figure 1.** Bodyweight before and after treatment.

3.1.2.2. The effect of thalixisosteres 3a--3f on kidney injury caused by I/R.

As illustrated in Figures 2 and 3. There was a significant increase in creatinine from all I/R treated with thalixisosteres **3a-3f** groups as compared to negative and positive control groups (P≤0.01). Also, there was an insignificant difference in creatinine from I/R treated with thalixisosteres **3a-3f** groups compared to I/R treated with thalix groups (P>0.05).

There was a significant increase in urea from all I/R treated with thalix and thalixisosteres **3a-3f** groups compared to negative control and positive control groups (P≤0.01). There were insignificant differences in urea from all I/R treated with thalixisosteres **3a-3f** groups as compared to thalix groups (P>0.05).

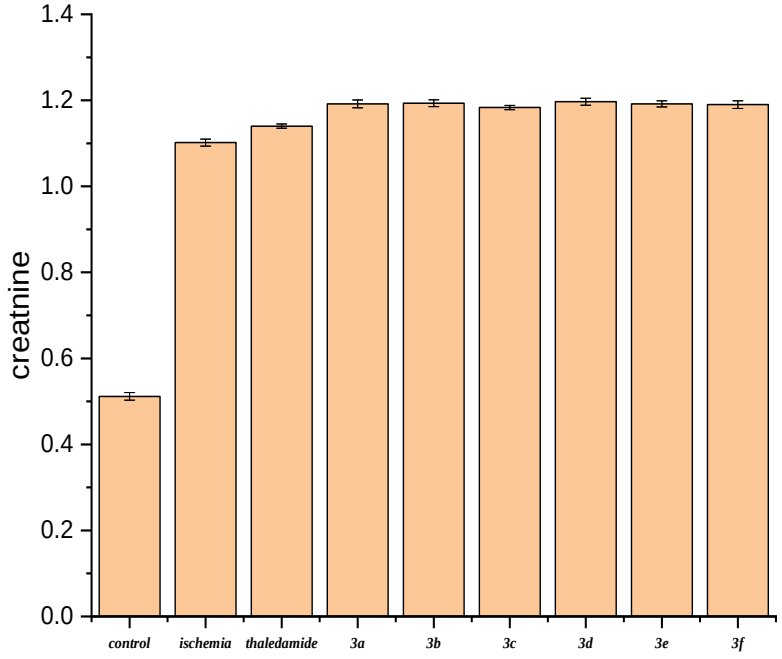


**Figure 2.** Level of serum creatinine in studied groups.

3.1.2.3. The effect of thalixisosteres 3a-3f on Oxidative stress.

As illustrated in Figure 4, there was a significant increase in the mean concentration of MDA in kidney tissue obtained from all I/R treated with thalix and thalixisosteres **3a-3f** groups

as compared to a negative control group (P≤0.01). The mean MDA concentrations in kidney tissue of all I/R treated with thalix and thalixisosteres **3a-3f** were significantly lower than that in positive control group (P≤0.01). Also, there was a significant increase in MDA concentrations in kidney tissue from I/R treated with thalixisosteres **3a-3e** groups as compared to I/R treated with thalixisosteres **3f** group (P≤0.05).

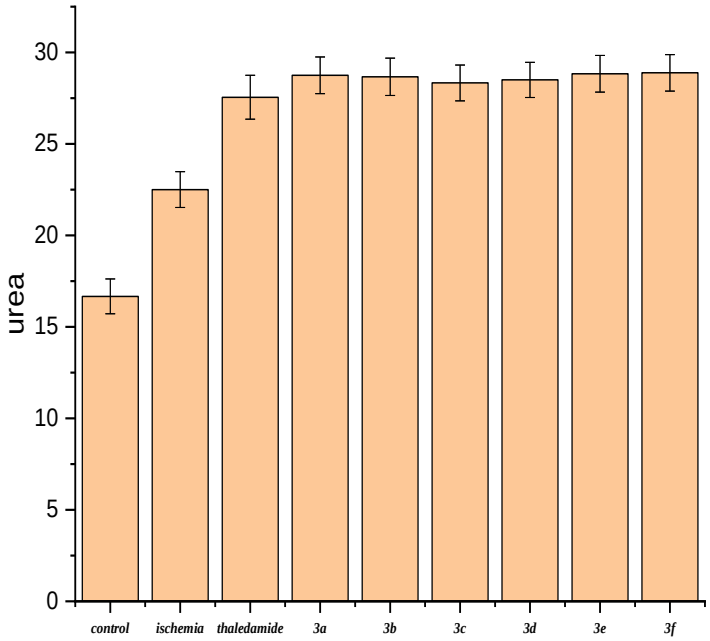


**Figure 3.** Serum urea in studied groups.

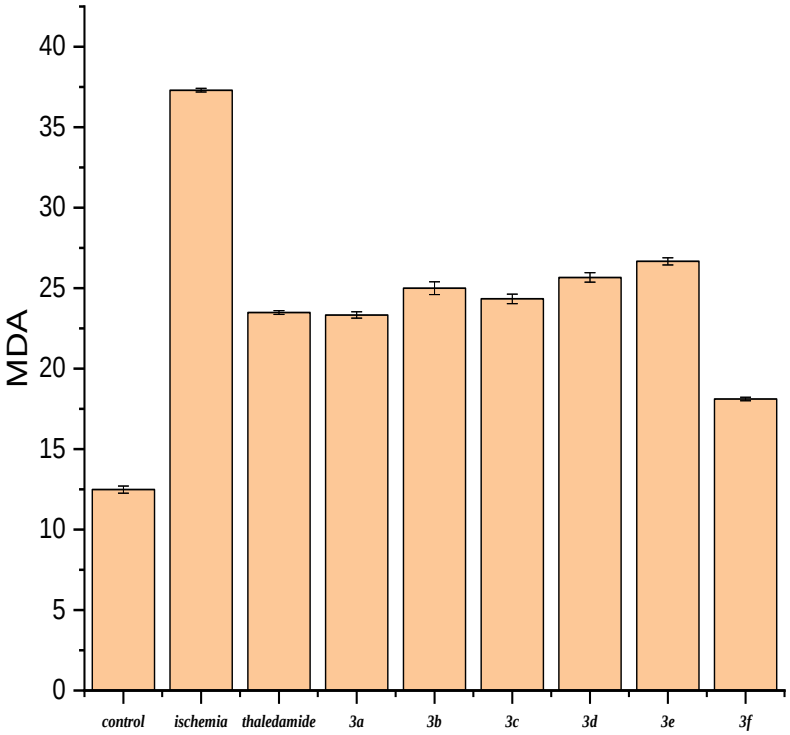


**Figure 4.** Level of MDA in studied groups.

As shown in Figure 5, there was a significant decrease in the mean concentrations of GSH in kidney tissue samples obtained from all I/R treated with thalix and thalixisosteres **3a-3f** groups compared to a negative control group (P ≤ 0.01). Moreover, there was a significant increase in the mean concentrations of GSH in kidney tissue samples from all I/R treated with

thalix and thalixisosteres **3a-3f** compared with positive control groups ($P \leq 0.01$). In addition, mean concentrations of GSH in kidney tissue of I/R treated with thalixisosteres **3a-3e** groups were significantly decreased compared to I/R treated with thalixisosteres **3f** group ($P \leq 0.01$).

As illustrated in Figure 6, there was a significant decrease in the mean activity of SOD in kidney tissue samples obtained from all I/R treated with thalix and thalixisosteres **3a-3f** groups compared to a negative control group ($P \leq 0.01$). Moreover, there was a significant increase in the mean activity of SOD in kidney tissue samples from all I/R treated with thalix and thalixisosteres **3a-3f** groups as compared with positive control groups ($P < 0.01$). In addition, the mean SOD activity in kidney tissue of I/R treated with thalixisosteres **3a-3e** groups was significantly decreased compared to I/R treated with thalixisosteres **3f** group ($P \leq 0.01$).

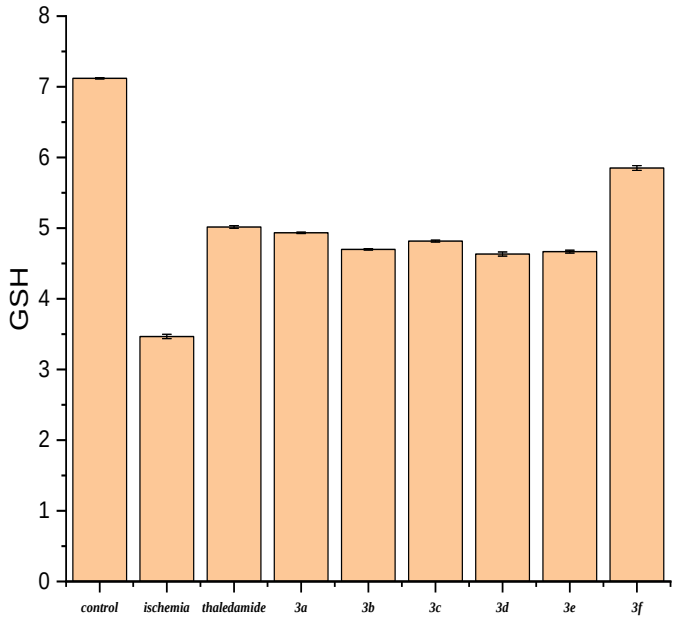


**Figure 5.** Level of **GSH** in studied groups.

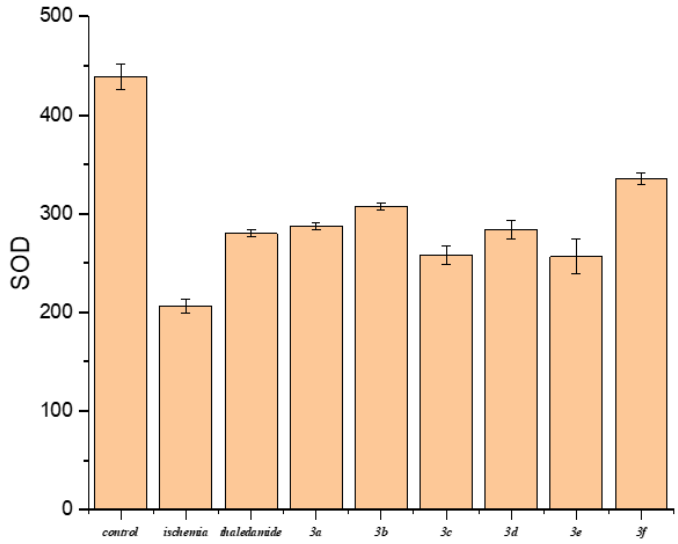


**Figure 6.** Level of **SOD** in studied groups.

3.1.2.4. The effect of thalixisostere 3f on angiogenesis.

As illustrated in Figure 7, there were insignificant differences in VEGF obtained from all I/R treated with thalix and thalixisosteres **3a-3e** groups compared to a negative control group

(P > 0.05). On the other hand, there were insignificant differences in VEGF from thalixisosteres **3a-3e** groups compared with thalix groups (P >0.05). Moreover, there was a significant decrease in the mean VEGF from I/R treated with thalixisosteres **3f** groups compared with negative and positive control groups (P ≤ 0.001). In addition, the mean concentrations of VEGF of I/R treated with thalixisosteres **3a-3e** groups were significantly increased compared to I/R treated with thalixisosteres **3f** group (P≤0.001).

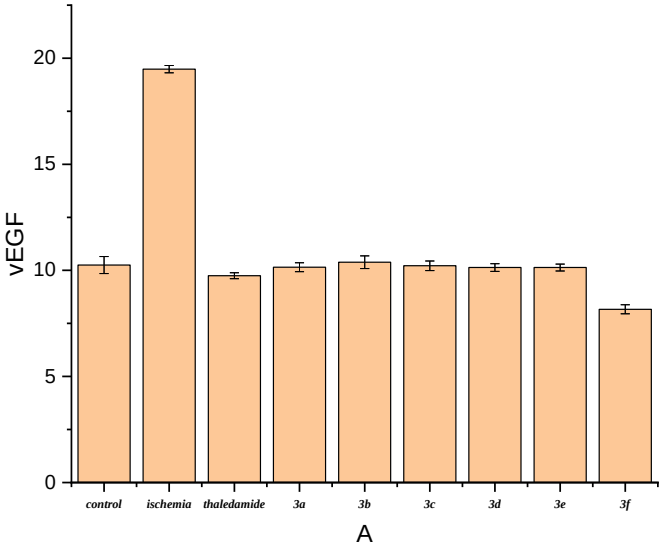


**Figure 7.** VEGF in studied groups.

3.2. Discussion.

Renal I/R injury is a complex inflammatory process in which the kidney is functionally and morphologically damaged during the ischemic phase and undergoes extra injury during reperfusion. In the present study, we used the Sprague-Dawley rat model of renal I/R injury (45 min) and observed it by renal function. The effect of pretreatment with thalix and new thalix on renal function and angiogenesis (VEGF), as well as on MDA (a marker of lipid peroxidation) and SOD (a marker of antioxidant enzyme) and GSH (a marker of non-enzymatic antioxidant) was investigated.

The present study showed a significant increase in serum creatinine and urea and a significant decrease in creatinine clearance at 3, 7, and 14 days after I/R, suggesting a significant degree of renal dysfunction. These findings confirm that I/R injury of the kidney causes glomerular dysfunctions and are in agreement with those reported previously [2]. According to the reported work [14], increased serum creatinine rates at the first 24 hours after reperfusion and the decrease on the $7^{th}$ day may increase muscle mass.

By thailx and new thalix treatment, there was a significant increase in creatinine and urea and a decrease in creatinine clearance. These findings confirm that minimal glomerular or tubular atrophy or necrotic changes were demonstrated in kidneys of thalidomide-treated rats with those reported previously [15].

In this study, treatment with thalix and new thalix for 3, 7, and 14 days reduces the expression of VEGF as compared to control groups (P=0.001). VEGF was markedly upregulated in the positive control group. This finding suggests that it is possible that the release of growth factors (VEGF), triggered by proinflammatory cytokines by which thalix reduced VEGF production [16].

The involvement of ROS in I/R injury to the kidney and other organs is widely accepted. As inflammation is associated with free radical production and oxidative stress, there was also an increase in lipid peroxidation level and a decrease in SOD and GSH levels in I//R injury models.

Oxidative stress injury of the kidney may play a major role in inducing remote organ injury. The involvement of ROS in I/R injury to the kidney and other organs is widely accepted. We examined oxidative stress state in kidney tissues during renal I/R injury. We found a significant increase in MDA concentration (a marker of lipid peroxidation) and catalase enzyme, and a significant decrease in GSH in the kidney tissues after renal I/R injury. These findings suggest increased oxidative stress in the kidney during renal I/R injury and support findings [2].

The first step in this work was to investigate the effect of new thalix on ROS at renal I/R injury. In the present study, thailx and new thalix treatment were associated with a significant decrease in MDA and a significant increase in the activity of SOD and GSH in kidney tissue in renal I/R injury. These findings verified that the new thalix might be capable of acting as a direct antioxidant as well by activating antioxidant defense mechanisms. To the best of our knowledge, the present study is the first to show the effects of new thalix in preventing oxidative stress in I/R-induced renal injury.

The next step in this work was to investigate the effect of new thalix on angiogenesis at renal I/R injury model. The effect of thalix and new thalix on renal I/R was also investigated; the mean concentrations of VEGF of new thalix treated groups were lower than that in thalix treated group rats ($P < 0.05$) on various days after I/R. Since VEGF is highly specific, a number of studies have reported that VEGF has an important role in promoting proliferation, migration, and chemotactic response in bone, lung, kidney, brain, vascular endothelial cells, tumor, and other tissues [17]. Therefore, the formation of new capillaries was also reduced. This may be associated with the thalix-induced downregulation of VEGF [18]. Thalidomide inhibits expression of the pro-angiogenic factors VEGF and basic fibroblast growth factor (bFGF) via mechanisms involving tumor necrosis factor-alpha (TNFalpha) and transcriptional activation of the VEGF promoter [19].

3.2.1. Structural similarity and docking affinity.

The difference in linearity and aromaticity between the two compounds was expressed in their degree of complementarity and interaction with the surrounding amino acids (Figure 8).

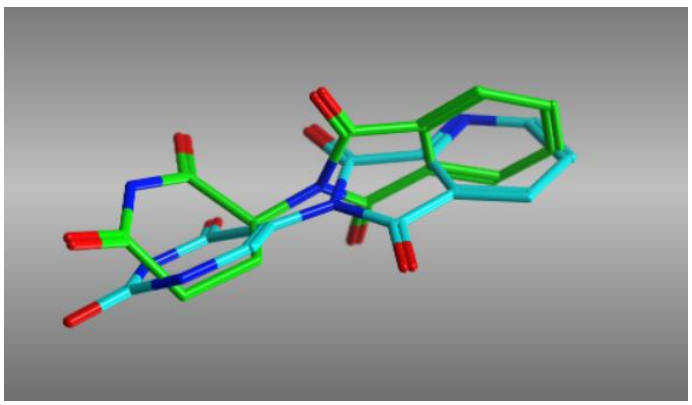

**Figure 8.** 3D sketch of both thalidomide (green colored) and the new compound (Blue colored) showing their docking layout. Heteroatoms colored Blue N and Red oxygen.

3.2.2. VEGFR binding active site.

The binding-active site of VEGFR2 has extensive recognition towards the proper active docked analogs via expressing stable hydrogen bonds with the key amino acid residues, namely; Glu885, Val899, Asp104.

3.2.3. Docking of thalidomide.

The thalidomide expressed unique recognition with the key amino acid residues that are laid towards function. *N*-piperidinedione showed a strong hydrogen bond with Val899. In comparison, the two carbonyl oxygens expressed proper recognitions with the corresponding Glu885 and Asp1046 through binding to two solvent molecules of water. (Figure 9).

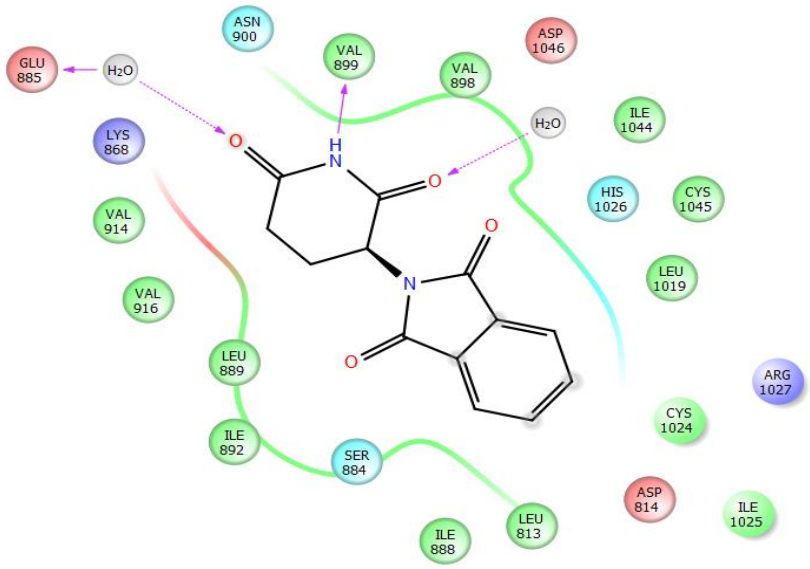


**Figure 9**. X-ray binding interaction of thalidomide within the binding pocket of VEGFR2 complex (code: 4ASD).

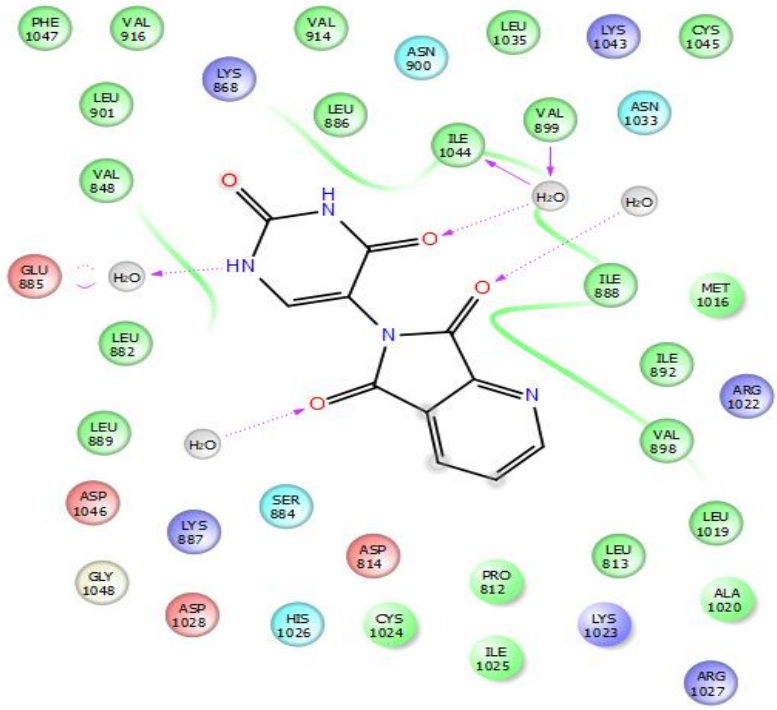


**Figure 10**. Putative binding mode of the new compound within the binding pocket of VEGFR.

3.2.4. Docking of thalidomide bioisostere.

Solvent expressed an exclusive role in recognition of the new compound within the VEGFR active site. The new compound expressed unique recognition with the key amino acid residue laid towards N1 of uracil expressed proper recognition with the corresponding Glu885 oxygen through binding to a water molecule.

Furthermore, carbonyl oxygen-4 showed strong bifurcated hydrogen bonds with both Val899 and Ile1044 through one solvent molecule.

Binding interaction with both carbonyl oxygens of the pyrrole ring was performed through binding to two molecules of water to be recognized properly with Asp1046 and Ile 888, respectively (Figure 10).

## 4. Conclusions

Consistent with the laboratory findings, this new thalix reduces VEGF formation at the three sample times. These findings suggest that new thalix is more effective than thalix in inhibiting the expression VEGF as pro-angiogenic factors. To the best of our knowledge, the present study is the first study to exhibit the antiangiogenic activity of new thalix in I/R-induced renal injury.

## Funding

This research received no external funding.

## Acknowledgments

The authors are grateful to Prof. Dr. Laila Abou Zeid, Professor of Pharmacology, Department of Pharmaceutical Chemistry, Faculty of Pharmacy, Mansoura University, Mansoura, Egypt, for supporting this work by molecular docking information.

## Conflicts of Interest

The authors declare no conflict of interest.

## References

1. Chueh, T.H.; Cheng, Y.H.; Chen, K.H.; Chien, C.T. Thromboxane A2 synthase and thromboxane receptor deletion reduces ischaemia/reperfusion-evoked inflammation, apoptosis, autophagy and pyroptosis. *Thrombosis and haemostasis* **2020**, *120*, 329-343, https://doi.org/10.1055/s-0039-3400304.
2. Hussein, A.E.-A.; Shokeir, A.A.; Sarhan, M.E.; El-Menabawy, F.R.; Abd-Elmoneim, H.A.; El-Nashar, E.M.; Barakat, N.M. Effects of combined erythropoietin and epidermal growth factor on renal ischaemia/reperfusion injury: a randomized experimental controlled study. *BJU Int.* **2011** ,*107*, 323-328, https://doi.org/10.1111/j.1464-410X.2010.09328.x.
3. Kato, E.T.; Kimura, T. Sodium-glucose co-transporters-2 inhibitors and heart failure: state of the art review and future potentials. *International Journal of Heart Failure* **2020**, *2*, 12-22, https://doi.org/10.36628/ijhf.2019.0013.
4. Nwafor, E.O.; Lu, P.; Li, J.W. Traditional Chinese medicine of Salvia miltiorrhiza Bunge: a review of phytochemistry, pharmacology and pharmacokinetics. *Tradit Med Res* **2021**, *6*, 35, https://doi.org/10.12032/TMR20201027204.
5. Xiao-Qing, Z.; Ke-Wu, Z. Advances in anti-inflammatory and immunoregulatory mechanisms of sinomenine. *Traditional Medicine Research* **2021**, *6*, 6, https://doi.org/10.12032/TMR20200814194.

6. Ashour, R.H.; Abd-Allah, M.A.; Mostafa, F.E.; Osman, B.H.; Kahter, Y.T.; El-Biomy, A.A.; El-Gilany, A.-H.A.; Saad, M.-A.A.; Sobh, M.A. Erythropoietin versus allopurinol on ischemia/reperfusioninduced acute kidney injury in rats. *Benha Med. J.* **2018**, *35*, 89-96, https://doi.org/10.4103/bmfj.bmfj_165_17.
7. Ali, S.S.; Noordin, L.; Bakar, R.A.; Zainalabidin, S.; Jubri, Z.; Ahmad, W.A.N.W. Current Updates on Potential Role of Flavonoids in Hypoxia/Reoxygenation Cardiac Injury Model. *Cardiovascular Toxicology* **2021**, *21*, 605–618, https://doi.org/10.1007/s12012-021-09666-x.
8. Zhang, X.; Luo, H. Effects of thalidomide on growth and VEGF-A expression in SW480 colon cancer cells. *Oncol. Lett.* **2018**, *15*, 3313–3320, https://doi.org/10.3892/ol.2017.7645.
9. Willems-Widyastuti, A.; Vanaudenaerde, B.M.; Vos, R.; Dilisen, E.; Verleden, S.E.; De Vleeschauwer, S.I.; Vaneylen, A.; Mooi, W.J.; de Boer, W.I.; Sharma, H.S.; Verleden, G.M. Azithromycin attenuates fibroblast growth induced vascular endothelial growth factor via p38MAPK signaling in human airway smooth muscle cells. *Cell Biochem. Biophys.* **2013**, *67*, 331–339, https://doi.org/10.1007/s12013-011-9331-0.
10. Ancidoni, A.; Bacigalupo, I.; Remoli, G.; Lacorte, E.; Piscopo, P.; Sarti, G.; Corbo, M.; Vanacore, N; Canevelli, M. Anticancer drugs repurposed for Alzheimer's disease: a systematic review. *Alzheimer's Research & Therapy* **2021**, *13*, 96, https://doi.org/10.1186/s13195-021-00831-6.
11. Fakhri, S.; Abbaszadeh, F.; Jorjani, M.; Pourgholami, M.H. The effects of anticancer medicinal herbs on vascular endothelial growth factor based on pharmacological aspects: a review study. *Nutrition and cancer* **2021**, *73*, 1-15, https://doi.org/10.1080/01635581.2019.1673451.
12. Dorrell, M.I.; Kast-Woelbern, H.R.; Botts, R.T.; Bravo, S.A.; Tremblay, J.R.; Giles, S.; Wada, J.F.; Alexander, M.; Garcia, E.; Villegas, G; Booth, C.B. A novel method of screening combinations of angiostatics identifies bevacizumab and temsirolimus as synergistic inhibitors of glioma-induced angiogenesis. *PloS one* **2021**, *16*, e0252233, https://doi.org/10.1371/journal.pone.0252233.
13. Fadda, A.A.; El-Gendy, E.; Refat, H.M.; Tawfik, E.H. Utility of dipyrromethane in the synthesis of some new $A_2B_2$ porphyrin and their related porphyrin like derivatives with their evaluation as antimicrobial and antioxidant agents. *Dyes and Pigments* **2021**, *191*, 109008, https://doi.org/10.1016/j.dyepig.2020.109008.
14. Leal, D.M.; Júnior, S.T.; Suaid, H.J.; Cologna, A.J.; Martins, A.C.P.; Roselino, J.E.S. Proteçãofuncional do rim com lovastatinaapósisquemia e reperfusão renal. *Acta Cir. Bras.* **2001**, *16*, 23-26, https://doi.org/10.1590/S0102-86502001000500009.
15. Shehata, A.H.; Ahmed, A.S.F.; Abdelrehim, A.B.; Heeba, G.H. The impact of single and combined PPAR-α and PPAR-γ activation on the neurological outcomes following cerebral ischemia reperfusion. *Life sciences* **2020**, *252*, 117679, https://doi.org/10.1016/j.lfs.2020.117679.
16. Akgun, Y.; Bakirdogen, S.; Kadioglu Kocak, M.G.; Bektas, S.; Demir, C.; Akbal, E.; Elmas, S. Efficacy of adalimumab therapy in experimental rat sclerosing encapsulated peritonitis model. *Croatian medical journal* **2019**, *60*, 431-438, https://doi.org/10.3325/cmj.2019.60.431.
17. Iacovelli, R.; Sternberg, C.; Porta, C.; Verzoni, E.; de Braud, F.; Escudier, B.; Procopio, G. Inhibition of the VEGF/VEGFR pathway improves survival in advanced kidney cancer: a systematic review and meta-analysis. *Curr. Drug Targets* **2015**, *16*, 164–170, https://doi.org/10.2174/1389450115666141120120145.
18. Chen, Y.; Cai, N.; Lai, Y.; Xu, W.; Li, J.; Huang, L.; Huang, Y.; Hu, M.; Yang, H.; Chen, J. Thalidomide for the Treatment of Thrombocytopenia and Hypersplenism in Patients with Cirrhosis or Thalassemia. *Frontiers in Pharmacology* **2020**, *11*, 1137, https://doi.org/10.3389/fphar.2020.01137.
19. Loreen, A.; Polen-De, C.; Monk, B.J.; Jackson, A.L.; Billingsley, C.C.; Herzog, T.J. The role of blinded independent radiologic review in ovarian cancer clinical trials: Discerning the value. *Gynecologic Oncology* **2021**, *161*, 491-495, https://doi.org/10.3322/caac.21590.